

Fully Spiking Neural Network for Legged Robots

Xiaoyang Jiang^{1,*}, Qiang Zhang^{2,*}, Jingkai Sun², Renjing Xu^{2,†}

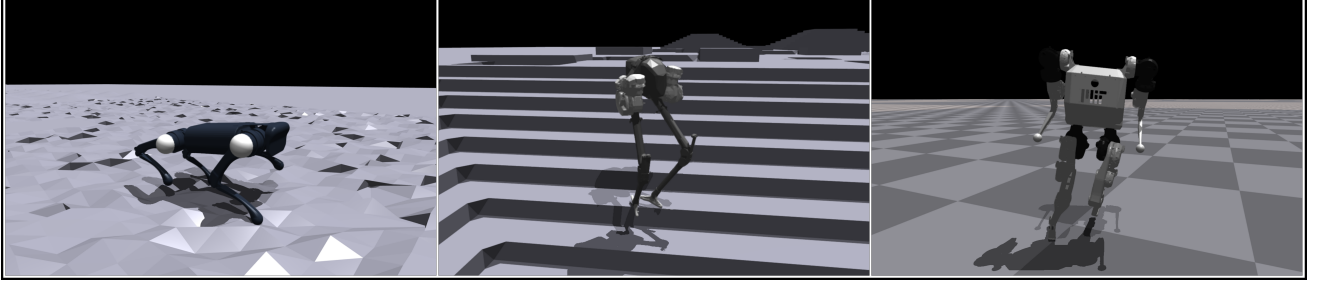


Fig. 1: Whole-body control on various types of robots through our spike-based approach. This innovative methodology allows us to effectively regulate and coordinate the robots' movements, enhancing their overall performance and versatility. **Left:** A1 **Middle:** Cassie **Right:** MIT Humanoid

Abstract—In recent years, legged robots based on deep reinforcement learning have made remarkable progress. Quadruped robots have demonstrated the ability to complete challenging tasks in complex environments and have been deployed in real-world scenarios to assist humans. Simultaneously, bipedal and humanoid robots have achieved breakthroughs in various demanding tasks. Current reinforcement learning methods can utilize diverse robot bodies and historical information to perform actions. However, prior research has not emphasized the speed and energy consumption of network inference, as well as the biological significance of the neural networks themselves. Most of the networks employed are traditional artificial neural networks that utilize multilayer perceptrons (MLP). In this paper, we successfully apply a novel Spiking Neural Network (SNN) to process legged robots, achieving outstanding results across a range of simulated terrains. SNN holds a natural advantage over traditional neural networks in terms of inference speed and energy consumption, and their pulse-form processing of body perception signals offers improved biological interpretability. To the best of our knowledge, this is the first work to implement SNN in legged robots.

I. INTRODUCTION

The increasing adoption of mobile robots, which are equipped with continuous high-dimensional observations and action space, to tackle a wide range of intricate tasks in real-world situations emphasizes the critical importance of exceptional control algorithms. Currently, the limited on-board energy resources of most robots pose a significant challenge, as this constraint hinders their ability to operate continuously and cost-effectively. Consequently, there is an immediate demand for developing energy-efficient solutions for the seamless control of these autonomous machines. Deep reinforcement learning (DRL) employs deep neural

networks (DNNs) as potent function approximators for learning optimal control strategies for intricate tasks [1], [2], through directly mapping the original state space to the action space [3], [4]. Nonetheless, the remarkable performance of DRL frequently comes at the expense of substantial energy consumption and slower execution speeds, making them unsuitable for various applications. Additionally, the execution speed of control strategies employing DNNs tends to be slower in comparison to the operational speed of the motion units. This discrepancy often results in a step-like behavior in the control signals, causing negative impacts on the performance of the system.

Spiking neural networks (SNNs), also referred to as third-generation neural networks, present a promising alternative for energy-efficient and high-speed deep networks. These emerging SNNs operate based on the principles of neuromorphic computing, wherein the integration of memory and computation is seamless, and neurons engage in asynchronous, event-based communication and computation [5]. The biological plausibility, the significant increase in energy efficiency (particularly when deployed on neuromorphic chips [6]), high-speed processing and real-time capability for high-dimensional data (especially from asynchronous sensors like event-based cameras [7]) contribute to the advantages that SNNs possess over ANNs in specific applications. These advantages render the utilization of SNNs not only feasible but also highly advantageous in lieu of ANNs for performing effective calculations. A mounting body of research illustrates that SNNs can function as energy-efficient and high-speed solutions for effectively managing robot control in scenarios where there are limitations on onboard energy resources [8]–[10]. To address the limitations of SNNs in tackling high-dimensional control problems, a natural approach involves combining the energy efficiency of SNNs with the optimality of DRL, which has proven effective in various control tasks [11]. Due to the role of rewards as training guides in reinforcement learning (RL), some studies

* are equal contributors, † is the corresponding author(renjingxu@ust.hk)

¹Xiaoyang Jiang is with Faculty of Robot Science and Engineering, Northeastern University, China

²The authors are with The Hong Kong University of Science and Technology (Guangzhou), China

utilize a three-factor learning rule [12] to implement reward learning. Although these rules exhibit strong performance in low-dimensional tasks, they often struggle to handle complex problems, and the optimization process becomes challenging in the absence of a global loss function [13]. Recently, [14] proposed a strategy gradient-based algorithm to train an SNN for learning random strategies. However, this algorithm is designed for discrete action spaces, and its practical applications are somewhat limited when tackling high-dimensional continuous control problems.

The recent conceptualization of the brain's topology and computational principles has ignited advancements in SNNs, exhibiting both human-like behavior [15] and superior performance [16]. A pivotal attribute associated with effective computation in the brain is the employment of neuronal populations for encoding and representing information, encompassing the entire spectrum from sensory input to output signals. In this scenario, each neuron within a population has a receptive field that captures a specific segment of the encoded signal [17]. Notably, initial investigations into this group coding scheme have shown its enhanced capability to represent stimuli [18], contributing to recent triumphs in training SNNs for complex, high-dimensional supervised learning tasks [19], [20]. The efficacy of population coding presents a promising pathway for the advancement of efficient SNNs that leverage population coding. These networks possess the potential to acquire optimal solutions for complex high-dimensional continuous control tasks, paving the way for significant progress in this field.

The main contributions of this paper can be summarized as follows:

- For the first time, we have implemented SNNs on a policy network in the legged robot simulated in Isaac Gym [21], enabling the encoding of each dimension of the observation and action space within a single population of neurons using a learnable acceptance domain. Furthermore, we have successfully integrated this method and achieved successful training outcomes using techniques such as imitation learning and trajectory history.
- We have decreased the decimation time to allow for more frequent updates during the learning process. Numerous experiments have consistently shown that SNNs perform exceptionally well even at ultra-high control frequencies.
- We achieved successful training on three typical legged robots: quadruped robotic dog a1, bipedal robot Cassie, and MIT humanoid, which fully demonstrate the feasibility and superiority of our method for application on legged robots (Fig. 1).

II. RELATED WORK

A. Reinforcement Learning for Legged Robotics Locomotion

In recent years, there has been a rapid development of reinforcement learning techniques in the realm of achieving fast, stable, and adaptive locomotion for legged robots. [22]

bridges the gap between reinforcement learning simulation and actual reality by modeling the actuator through neural networks. [23] utilizes the teacher-student training framework to integrate environmental parameters with preconceptions which enables quadruped robots to adapt to complex terrains. [24] introduces a large number of auxiliary rewards and gait parameter control to implement multiple gaits for a single policy. This work brings a lot of inspiration to the design of quadruped rewards. [25] combines reinforcement learning with computer vision to complete simultaneous locomotion and manipulation. Unlike traditional reinforcement learning, Generative adversarial imitation learning (GAIL) is an approach for imitating behaviors from reference datasets by integrating a generative adversarial network. Based on the GAIL, Adversarial Motion Priors (AMP) combines the task reward and imitation reward to make the agent complete the tasks based on the action being similar to the reference dataset. For learning unlabeled references dataset, [26] uses a skill discriminator additionally and enables quadruped to distinguish and master multiple gaits, and perform backflips not found in the dataset. [27] combines RMA and AMP, allowing the quadruped with the ability to traverse challenging terrains rapidly. However, the above methods are realized by ANNs. Therefore, it cannot take into account the high-frequency and energy-saving advantages of SNNs.

B. Spiking Neuron Networks

Recently, many works have grown up around introducing SNNs into RL algorithms [12], [28]–[31]. SNNs offer advantages in processing temporal information, energy efficiency, event-driven processing, robustness to noise, plasticity, and biological plausibility. Some methods get trained ANNs to be converted into corresponding SNNs with few accuracy loss by matching the firing rates of spiking neurons with the graded activation of analog neurons [32].

Yet following the surrogate gradient method [33], the spike-based backpropagation (BP) algorithm has quickly become the mainstream solution for training multi-layer SNNs [34]. As shown in several open-source frameworks of SNNs [35], [36], the membrane voltage of non-spiking neurons is feasible to represent a continuous value in a spike-based BP method.

III. SNNs BASED LOCOMOTION IN ISAACGYM

We chose to train and test the performance of our algorithm on Isaac Gym [21]. Isaac Gym is a simulation platform designed for robotics. It offers realistic physics simulation, specialized support for legged robots, integration with NVIDIA technologies, customization options, and an active community.

A. SNN based Policy Network

We utilize a population-coded spiking actor-network (PopSAN) [37] that is trained in conjunction with a deep critic network using the DRL algorithms (including RMA and AMP). During training, the PopSAN generated an action $\alpha \in \mathbb{R}^N$ for a given observation, s , and the deep critic network

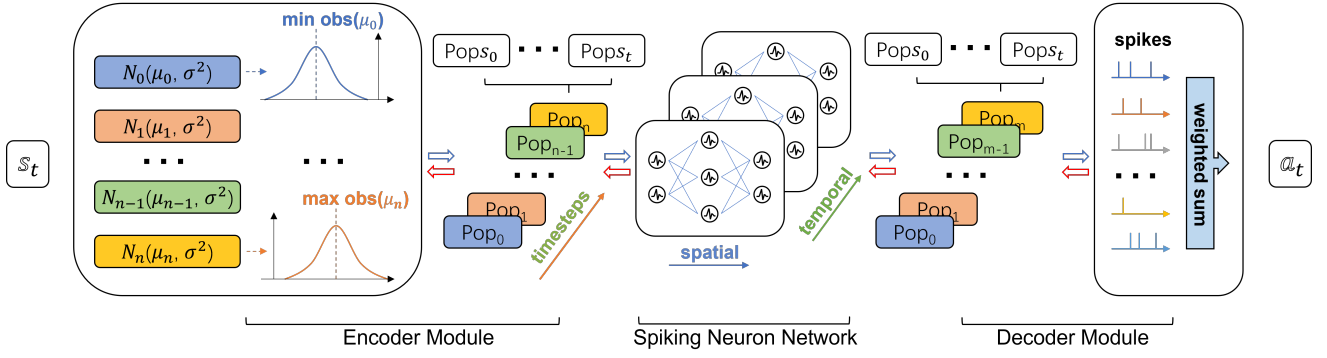


Fig. 2: Firstly, the observations are encoded by the encoder as n independent distributions, uniformly distributed over the range of the observation. These encoded distributions are then further processed by the population, resulting in the generation of the corresponding spikes. Then the neurons in the input populations are responsible for encoding each dimension of the observation and they drive a multi-layered and fully connected SNN. During the forward timesteps, the activities of each output population in PopSAN are decoded to determine the corresponding action dimension. This means that the neural network takes in observations, processes them through the SNN, and then decodes the resulting activities to generate the appropriate action for the given situation.

Algorithm 1 Forward propagation through PopSAN

Randomly initialize weight matrices \mathbf{W} and biases \mathbf{b} for each SNN layer;
Initialize encoding means μ and standard deviations σ for all input populations;
Randomly initialize decoding weight vectors \mathbf{W}_d and bias b_d for each action dimension;
 N -dimensional observation, \mathbf{s} ;
Spikes from input populations generated by encoder module: $\mathbf{X} = \text{Encoder}(\mathbf{s}, \mu, \sigma)$;
for $t = 1, \dots, T$ **do**
 Spikes at timestep t : $\mathbf{o}^{(t)(0)} = \mathbf{X}^{(t)}$;
 for $k = 1, \dots, K$ **do**
 Update LIF neurons in layer k at timestep t based on spikes from layer $k - 1$:
 $\mathbf{c}^{(t)(k)} = d_c \cdot \mathbf{c}^{(t-1)(k)} + \mathbf{W}^{(k)} \mathbf{o}^{(t)(k-1)} + \mathbf{b}^{(k)}$;
 $\mathbf{v}^{(t)(k)} = d_v \cdot \mathbf{v}^{(t-1)(k)} \cdot (1 - \mathbf{o}^{(t-1)(k)}) + \mathbf{c}^{(t)(k)}$;
 $\mathbf{o}^{(t)(k)} = \text{Threshold}(\mathbf{v}^{(t)(k)})$;
 end for
end for
 M -dimensional action \mathbf{a} generated by decoder module:
Sum up the spikes of output populations: $\mathbf{sc} = \sum_{t=1}^T \mathbf{o}^{(t)(K)}$;
for $i = 1, \dots, M$ **do**
 Compute firing rates of the i^{th} output population:
 $\mathbf{fr}^{(i)} = \mathbf{sc}^{(i)} / T$;
 Compute i^{th} dimension of action: $\alpha^i = \mathbf{W}_d^{(i)} \cdot \mathbf{fr}^{(i)} + b_d^{(i)}$;
end for

predicted the associated state value $V(s)$ or action-value $Q(s, \alpha)$, which in turn optimized the PopSAN, in accordance with a chosen DRL method (Fig. 2). In the PopSAN architecture, the encoder module encodes each dimension of the observation into the activity of a specific neuron population. During forward propagation, these input populations stimulate a multi-layer fully-connected SNN. The SNN then produces activity patterns in the output populations. At the end of

every T timesteps, these activity patterns are decoded to determine the corresponding action dimensions (as outlined in Algorithm 1).

To construct the SNN, the current-based leaky-integrate-and-fire (LIF) model of a spiking neuron is employed. This model is utilized for building the SNN architecture. The dynamics of the LIF neurons are controlled by a two-step model, as elaborated in Algorithm 1: i) integrating the presynaptic spikes \mathbf{o} into current \mathbf{c} ; and ii) integrating the current \mathbf{c} into membrane voltage \mathbf{v} ; d_c and d_v are the current and voltage decay factors. In this implementation, a neuron fires a spike when its membrane potential surpasses a certain threshold. We adopted the hard-reset model, which means that upon spiking, the membrane potential is instantly reset to the resting potential. The resulting spikes are then transmitted to the post-synaptic neurons within the same inference timestep, assuming zero propagation delay. This approach enables efficient and synchronous transmission of information within the SNN.

Next, we combined the superiority of snn with the recently advanced algorithm RMA. Figure 3 illustrates that RMA system comprises two interconnected subsystems: the base policy π and the adaptation module ϕ , which collaborate harmoniously to facilitate continuous adaptation in a wide variety of environmental setups, thereby enabling smooth and uninterrupted online operations. The base policy is trained through reinforcement learning in simulation, utilizing privileged information about the environment configuration e_t , which includes factors like friction, payload, and more. By leveraging the knowledge of the vector e_t , the base policy can effectively adapt to the specific characteristics of the given environment. The process begins by encoding the environment configuration vector e_t into a latent feature space z_t through an encoder network μ . This latent vector, referred to as the extrinsics, is then combined with the current state x_t and the previous action α_{t-1} as inputs to the base policy. The base policy then generates predictions for the desired joint positions of the robot, denoted as a_t . The policy π and the environmental factor encoder μ undergo a collaborative training process using RL within a simulated

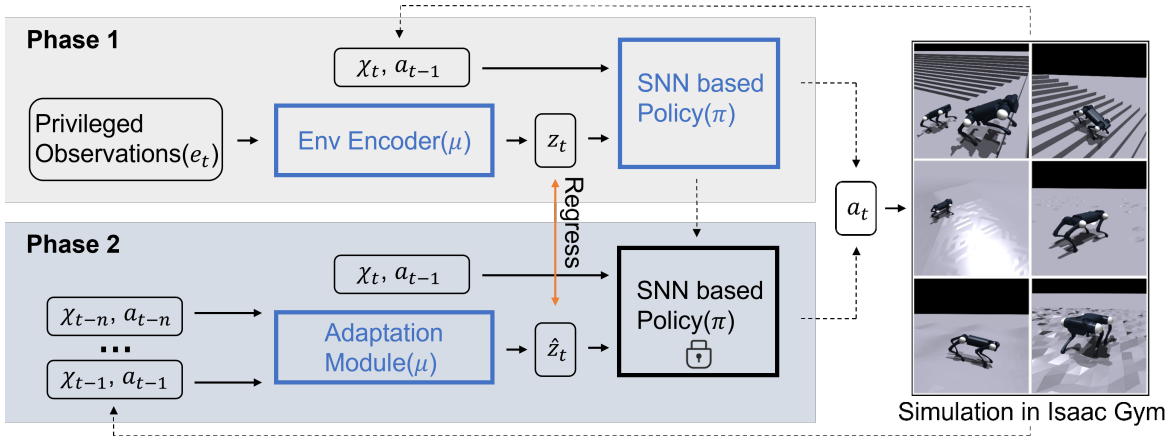


Fig. 3: RMA is a system composed of two subsystems: the base policy π and the adaptation module ϕ . The training of RMA consists of two phases. **Training the Base Policy (Phase 1):** In the first phase, the base policy π is trained using PopSAN. It takes as input the current state x_t , the previous action a_{t-1} , and the privileged environmental factors e_t . These environmental factors are encoded into a latent extrinsics vector z_t using the environmental factor encoder μ . **Training the Adaptation Module (Phase 2):** In the second phase, the adaptation module ϕ is trained to predict the extrinsics \hat{z}_t based on the history of states and actions. This training is done using supervised learning with on-policy data. The adaptation module learns to capture the relationship between the state-action history and the corresponding extrinsics. By training the base policy and the adaptation module in these two phases, RMA is able to learn and adapt to the environment in a more effective manner.

environment.

Regrettably, direct deployment of this policy is not feasible in the real world due to the unavailability of e_t . To overcome this challenge, we need to estimate the extrinsics during runtime, a task performed by the adaptation module ϕ . The key insight here is that when we instruct the robot joints to perform a specific movement, the actual movement executed deviates from the intended movement, and this deviation is influenced by the extrinsics. Rather than relying on privileged information, we can leverage the recent history of the agent’s state to estimate the extrinsics vector. Specifically, the purpose of ϕ is to estimate the extrinsics vector z_t solely based on the recent state and action history of the robot, without any direct access to e_t . At training time, since both the state history and the extrinsics vector z_t can be computed in simulation, we can train this module using supervised learning techniques.

In addition, we have successfully combined SNN with AMP and achieved similar performance to ANN on legged robots. Figure 4 provides a schematic overview of the system. The motion dataset M consists of a collection of reference motions, where each motion $m^i = \hat{q}_t^i$ is represented as a sequence of poses \hat{q}_t^i . The motion clips can be obtained from a variety of sources, including motion capture (mocap) recordings of real-life actors or artist-authored keyframe animations. The motion of the simulated robot is controlled by a policy $\pi(\alpha_t | s_t, g)$ that maps the state of the character s_t and a given goal g to a distribution over actions α_t . The actions generated by the policy dictate the desired target positions for proportional-derivative (PD) controllers, which are located at each joint of the robot. These controllers then generate control forces that propel the robot’s motion in accordance with the specified target positions. The goal g specifies a task reward function $r_t^G = r^G(s_t, \alpha_t, s_{t+1}, g)$, which defines high-level objectives that the robot must fulfill. These objectives can include tasks such as walking in a specific direction or executing a punch towards a designated

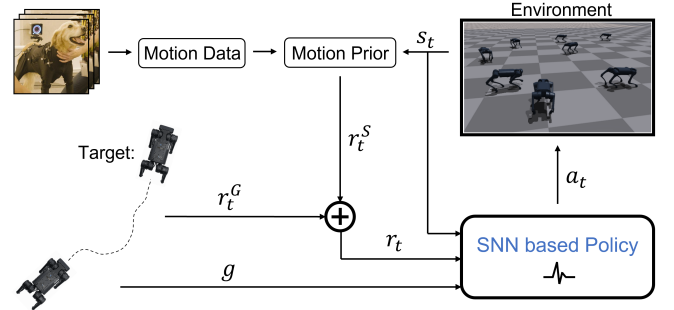


Fig. 4: By leveraging Adversarial Motion Priors and employing PopSAN as a replacement for the policy network during training, the agent is able to generate behaviors that capture the essence of the motion capture dataset.

target. The style objective $r_t^S = r^S(s_t, s_{t+1})$ is specified by an adversarial discriminator, trained to discern between motions captured in the dataset and motions generated by the robot itself. The style objective serves as a task-agnostic motion prior, offering an a-priori estimate of the naturalness or style of a given motion, regardless of the specific task. By doing so, the style objective motivates the policy to generate motions that closely resemble the behaviors observed in the dataset.

B. Training of Legged Robot using SNN on Isaacgym

In our study, we employed gradient descent to update the PopSAN parameters, where the exact loss function varies depending on the chosen algorithm (RMA or AMP). To train the parameters of PopSAN, we utilize the gradient of the loss with respect to the computed action, denoted as $\nabla_a L$. The parameters for each output population $i, i \in 1, \dots, M$ are updated independently as follows:

$$\nabla_{W_d^{(i)}} L = \nabla_{\alpha_i} L \cdot W_d^{(i)} \cdot \mathbf{f} \mathbf{r}^{(i)}, \nabla_{b_d^{(i)}} L = \nabla_{\alpha_i} L \cdot W_d^{(i)} \quad (1)$$

The SNN parameters are updated using the extended spatiotemporal backpropagation introduced in [38]. We used

TABLE I: Ranges of the environmental parameters

Parameters	Training range	Testing range
Friction	[0.005, 4.5]	[0.004, 6.0]
K_p	[50, 60]	[45, 65]
K_d	[0.4, 0.8]	[0.3, 0.9]
Payload(Kg)	[0, 6]	[0, 7]
Center of Mass(cm)	[-0.15, 0.15]	[-0.18, 0.18]
Motor Strength	[0.90, 1.10]	[0.88, 1.22]
Re-sample Probability	0.004	0.01

the rectangular function $z(v)$, defined in [39], to approximate the gradient of a spike. The gradient of the loss with respect to the SNN parameters for each layer k are computed by collecting the gradients backpropagated from all the timesteps:

$$\nabla_{\mathbf{W}^{(k)}} L = \sum_{t=1}^T \mathbf{o}^{(t)(k-1)} \cdot \nabla_{\mathbf{c}^{(t)(k)}} L, \nabla_{\mathbf{b}^{(k)}} L = \sum_{t=1}^T \nabla_{\mathbf{c}^{(t)(k)}} L \quad (2)$$

Lastly, we updated the parameters independently for each input population $i, i \in 1, \dots, N$ as follows:

$$\begin{aligned} \nabla_{\boldsymbol{\mu}^{(i)}} L &= \sum_{t=1}^T \nabla_{\mathbf{o}_i^{(t)(o)}} L \cdot \mathbf{A}_E^{(i)} \cdot \frac{s_i - \boldsymbol{\mu}^{(i)}}{\boldsymbol{\sigma}^{(i)^2}}, \\ \nabla_{\boldsymbol{\sigma}^{(i)}} L &= \sum_{t=1}^T \nabla_{\mathbf{o}_i^{(t)(o)}} L \cdot \mathbf{A}_E^{(i)} \cdot \frac{(s_i - \boldsymbol{\mu}^{(i)})^2}{\boldsymbol{\sigma}^{(i)^3}} \end{aligned} \quad (3)$$

IV. EXPERIMENTS

The goals of our experiments are the followings: i) To validate the feasibility of SNNs on robots with high-latitude complex environments and complex dynamics models. ii) Verify the advantages of SNNs over ANNs in terms of ultra-high flatness control. iii) Identify rewards that SNNs excel on rl tasks and make improvements on poorly performing rewards. We evaluated our method on the Isaac Gym with accurate physics simulation and flexible and customizable framework for robot models and environments.

We mainly tested the performance of the following robots: A1, Cassie and MIT Humanoid where each snn is trained within 1,500,000 iterations until convergence. The final visualization and metrics such as base velocity x, y, yaw, mean episode length and position torque are used for evaluation.

A. Simulation Setup

To create a diverse range of environments, we imported several URDF files from recent works. These files include models such as A1, Anyman-b, Anyman-c, Cassie, MIT Humanoid, and more. Once imported, we leverage the capabilities of the Isaac Gym simulator to create new environments for each of these models. To add variety, we make use of the inbuilt fractal terrain generator provided by the simulator. This terrain generator enables us to generate different types of terrain, ranging from plain terrains to uneven terrains with various topographical features. Our policy operates at a control frequency of up to 500Hz, due to our SNN-based

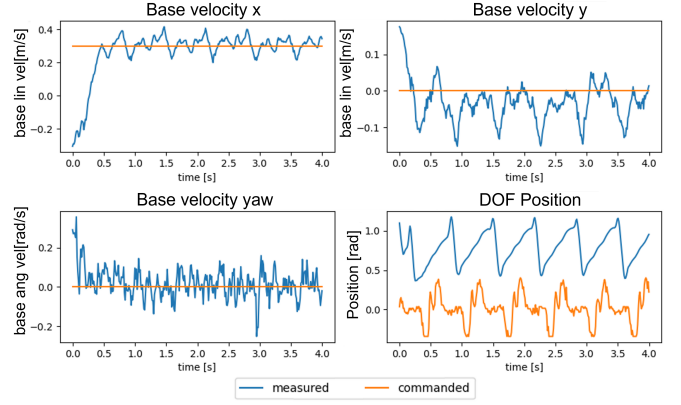


Fig. 5: The four graphs depicting the robot's x-axis linear velocity, y-axis linear velocity, yaw-axis angular velocity, and DOF position vividly demonstrate the successful accomplishment of the task through the implementation of our method.

approach. This allows us to achieve high-frequency control, resulting in fast and accurate adjustments to the system. In Table I listed a comprehensive list of environmental variations and their ranges.

B. Performances of High Frequency Control using SNNs

We conducted tests on the robots mentioned above specifically for linear and angular velocity tracking tasks. In these tests, we considered tracking velocity (linear and angular) as the primary positive rewards. Additionally, we incorporated penalties for base height that is too low, excessive acceleration, and instances where the robot falls, etc.

1) A1: For A1, we conducted training and testing in several terrain environments, including pyramid stairs like terraces (upstairs and downstairs), pyramids with sloping surfaces, hilly terrains, terrains with discrete obstacles, and terrains covered with stepping stones. On the other hand, Cassie is solely trained in a trapezoidal pyramid environment and MIT Humanoid in a plain terrain.

To further investigate the advantages of SNNs in high-frequency control scenarios, we deliberately increased the simulation environment's time step (dt) to 2.5 times the original default ANNs task, resulting in a frequency of 500Hz. By comparing the performance of SNN with ANN under these conditions, our aim is to establish whether SNN outperforms ANN in real-world environment that require high-frequency control.

The rationale behind this investigation stems from the fact that robots using ANN control algorithms often face limitations due to their onboard energy constraints. As a result, these robots can typically achieve only a policy inference frequency of 100Hz, which falls significantly behind the execution frequency of the motors. Conversely, SNN offers the potential to enhance the quality of policy inference and deliver more real-time control performance due to its energy-efficient nature and deployment on specialized processors. If SNN can achieve similar or even superior performance compared to ANN under high-frequency control, it would indicate the superiority of SNN in real-world environments.

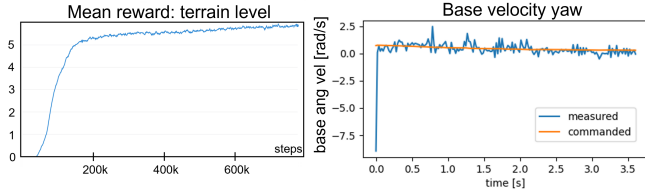


Fig. 6: The first image showcases Cassie’s remarkable capability to conquer complex terrain, as indicated by the terrain level value nearing 6. Additionally, the second figure demonstrates Cassie’s impeccable tracking of the angular velocity of the yaw axis, exemplifying its capacity to maintain body stability while traversing complex terrain.

In Figure 5, the effectiveness of our method under high-frequency control is clearly demonstrated. The performance of the A1 robot in tracking velocity x is highly commendable, showcasing its ability to accurately follow the desired trajectory. Moreover, when considering the impact of the intricate terrain environment, the fluctuation range of the linear velocity in the y -axis direction remains within an acceptable range. This further highlights the robustness of our method in tackling challenging terrains.

Furthermore, the results obtained in the yaw-axis angular velocity tracking are also notable. Although occasional spikes occur, indicating moments when the robot deviates from the existing policy framework, these instances can be attributed to the robot’s inclination to explore alternative approaches when faced with difficult terrain. This adaptive behavior showcases the robot’s ability to go beyond pre-existing policies and dynamically adapt its actions to overcome obstacles.

2) *Cassie*: The training results of Cassie robot have proven to be highly successful, as evidenced by the findings depicted in Figure 6. The stability observed in the angular velocity following along the yaw axis is particularly noteworthy. This stability is crucial in ensuring effective control and balance while navigating diverse terrains. Furthermore, the robot’s impressive ability to reach the highest level of terrain height, as indicated by a reward score of up to 6 (with each unit representing a layer in the pyramid ladder), showcases its adaptability in conquering rugged landscapes. These findings highlight the Cassie robot’s capacity to successfully traverse challenging terrains under the high control frequency of SNNs while maintaining stability and elegance. Consequently, the feasibility of our approach is substantiated, affirming its potential deployment in complex and ever-changing real-world scenarios.

3) *MIT Humanoid*: The training of MIT Humanoid also proved to be highly successful, showcasing the effectiveness of our spike-based approach. While it did take slightly longer to train compared to the traditional ANNs, the results obtained are equally impressive. In fact, they even surpassed the ANN in certain individual metrics, as clearly depicted in Figure 7. These findings strongly suggest that the SNN possesses inherent advantages when it comes to control robustness. Furthermore, it enables agents to not only thrive but also endure in their environment for an extended duration. This highlights the potential of SNN as a powerful tool in

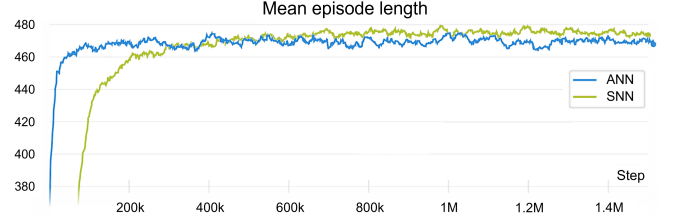


Fig. 7: In experiments conducted on the MIT Humanoid, the SNN achieves a comparable level of approximation with ANN in multiple evaluation metrics and even surpasses ANN. Despite the fact that SNN takes longer to train, the SNN outperforms ANN in terms of mean episode length after training convergence, providing strong evidence for the exceptional robustness of our method in whole body control.

enhancing agent performance and longevity.

In the videos presented, the robots trained using SNN-based policies exhibit remarkable characteristics, including smooth, stable, and natural gaits. Whether it is the agile traversal of challenging terrains by A1 and Cassie or the unrestricted running of the MIT Humanoid, the performance showcased by our approach is undeniably superior. Notably, the low energy consumption associated with SNN further positions it as a promising alternative to ANN. With its ability to achieve exceptional performance and energy efficiency, SNN holds great potential in the field of robotics.

V. CONCLUSION AND LIMITATION

This study presents the integration of PopSAN with two cutting-edge reinforcement learning techniques, namely history trajectory and imitation learning. This innovative approach enables SNNs to achieve performance comparable to ANNs. The successful training of SNN-based policy networks using these methods highlights the versatility of SNNs in policy gradient-based DRL algorithms, thereby opening up new horizons for their application in various reinforcement learning tasks, including continuous control.

Additionally, the study explores the suitability of SNNs for high-frequency control tasks, demonstrating that agents powered by SNNs can devise exceptional strategies even at an elevated inference frequency of 500Hz. These findings emphasize the advantages of SNN-based control methods over ANNs, particularly in scenarios with limited computational resources. They showcase the remarkable energy efficiency and robustness of SNNs, highlighting their potential in various applications.

However, due to the difficulty in obtaining neuromorphic chips, our experiments could not be conducted on a physical machine, consequently slightly diminishing the strength of our argument regarding the energy efficiency of SNNs.

By embracing SNNs, we unlock a realm of possibilities for future advancements in intelligent control systems, transcending traditional computational paradigms.

ACKNOWLEDGMENT

The authors would like to express their gratitude to Jingtong Ma and Chao Chen for their valuable contributions and insightful discussions.

REFERENCES

- [1] S. Ha, J. Kim, and K. Yamane, "Automated deep reinforcement learning environment for hardware of a modular legged robot," in *2018 15th international conference on ubiquitous robots (UR)*. IEEE, 2018, pp. 348–354.
- [2] Y. Zhu, R. Mottaghi, E. Kolve, J. J. Lim, A. Gupta, L. Fei-Fei, and A. Farhadi, "Target-driven visual navigation in indoor scenes using deep reinforcement learning," in *2017 IEEE international conference on robotics and automation (ICRA)*. IEEE, 2017, pp. 3357–3364.
- [3] Y. Duan, X. Chen, R. Houthoof, J. Schulman, and P. Abbeel, "Benchmarking deep reinforcement learning for continuous control," in *International conference on machine learning*. PMLR, 2016, pp. 1329–1338.
- [4] T. P. Lillicrap, J. J. Hunt, A. Pritzel, N. Heess, T. Erez, Y. Tassa, D. Silver, and D. Wierstra, "Continuous control with deep reinforcement learning," *arXiv preprint arXiv:1509.02971*, 2015.
- [5] M. Davies, N. Srinivasa, T.-H. Lin, G. Chinya, Y. Cao, S. H. Choday, G. Dimou, P. Joshi, N. Imam, S. Jain *et al.*, "Loihi: A neuromorphic manycore processor with on-chip learning," *Ieee Micro*, vol. 38, no. 1, pp. 82–99, 2018.
- [6] K. Roy, A. Jaiswal, and P. Panda, "Towards spike-based machine intelligence with neuromorphic computing," *Nature*, vol. 575, no. 7784, pp. 607–617, 2019.
- [7] G. Gallego, T. Delbrück, G. Orchard, C. Bartolozzi, B. Tabá, A. Censi, S. Leutenegger, A. J. Davison, J. Conradt, K. Daniilidis *et al.*, "Event-based vision: A survey," *IEEE transactions on pattern analysis and machine intelligence*, vol. 44, no. 1, pp. 154–180, 2020.
- [8] G. Tang, A. Shah, and K. P. Michmizos, "Spiking neural network on neuromorphic hardware for energy-efficient unidimensional slam," in *2019 IEEE/RSJ International Conference on Intelligent Robots and Systems (IROS)*. IEEE, 2019, pp. 4176–4181.
- [9] T. Taunayazov, W. Sng, H. H. See, B. Lim, J. Kuan, A. F. Ansari, B. C. Tee, and H. Soh, "Event-driven visual-tactile sensing and learning for robots," *arXiv preprint arXiv:2009.07083*, 2020.
- [10] C. Michaelis, A. B. Lehr, and C. Tetzlaff, "Robust trajectory generation for robotic control on the neuromorphic research chip loihi," *Frontiers in neurobotics*, vol. 14, p. 589532, 2020.
- [11] V. Mnih, K. Kavukcuoglu, D. Silver, A. A. Rusu, J. Veness, M. G. Bellemare, A. Graves, M. Riedmiller, A. K. Fidjeland, G. Ostrovski *et al.*, "Human-level control through deep reinforcement learning," *nature*, vol. 518, no. 7540, pp. 529–533, 2015.
- [12] N. Frémaux, H. Sprekeler, and W. Gerstner, "Reinforcement learning using a continuous time actor-critic framework with spiking neurons," *PLoS computational biology*, vol. 9, no. 4, p. e1003024, 2013.
- [13] R. Legenstein, C. Naeger, and W. Maass, "What can a neuron learn with spike-timing-dependent plasticity?" *Neural computation*, vol. 17, no. 11, pp. 2337–2382, 2005.
- [14] B. Rosenfeld, O. Simeone, and B. Rajendran, "Learning first-to-spike policies for neuromorphic control using policy gradients," in *2019 IEEE 20th International Workshop on Signal Processing Advances in Wireless Communications (SPAWC)*. IEEE, 2019, pp. 1–5.
- [15] P. Balachandrar and K. P. Michmizos, "A spiking neural network emulating the structure of the oculomotor system requires no learning to control a biomimetic robotic head," in *2020 8th IEEE RAS/EMBS International Conference for Biomedical Robotics and Biomechatronics (BioRob)*. IEEE, 2020, pp. 1128–1133.
- [16] R. Kreiser, A. Renner, V. R. Leite, B. Serhan, C. Bartolozzi, A. Glover, and Y. Sandamirskaya, "An on-chip spiking neural network for estimation of the head pose of the icub robot," *Frontiers in Neuroscience*, vol. 14, p. 551, 2020.
- [17] A. P. Georgopoulos, A. B. Schwartz, and R. E. Kettner, "Neuronal population coding of movement direction," *Science*, vol. 233, no. 4771, pp. 1416–1419, 1986.
- [18] G. Tkačik, J. S. Prentice, V. Balasubramanian, and E. Schneidman, "Optimal population coding by noisy spiking neurons," *Proceedings of the National Academy of Sciences*, vol. 107, no. 32, pp. 14419–14424, 2010.
- [19] G. Bellec, D. Salaj, A. Subramoney, R. Legenstein, and W. Maass, "Long short-term memory and learning-to-learn in networks of spiking neurons," *Advances in neural information processing systems*, vol. 31, 2018.
- [20] Z. Pan, J. Wu, M. Zhang, H. Li, and Y. Chua, "Neural population coding for effective temporal classification," in *2019 International Joint Conference on Neural Networks (IJCNN)*. IEEE, 2019, pp. 1–8.
- [21] V. Makoviychuk, L. Wawrzyniak, Y. Guo, M. Lu, K. Storey, M. Macklin, D. Hoeller, N. Rudin, A. Allshire, A. Handa *et al.*, "Isaac gym: High performance gpu-based physics simulation for robot learning," *arXiv preprint arXiv:2108.10470*, 2021.
- [22] J. Hwangbo, J. Lee, A. Dosovitskiy, D. Bellicoso, V. Tsounis, V. Koltun, and M. Hutter, "Learning agile and dynamic motor skills for legged robots," *Science Robotics*, vol. 4, no. 26, p. eaau5872, 2019.
- [23] A. Kumar, Z. Fu, D. Pathak, and J. Malik, "Rma: Rapid motor adaptation for legged robots," *arXiv preprint arXiv:2107.04034*, 2021.
- [24] G. B. Margolis and P. Agrawal, "Walk these ways: Tuning robot control for generalization with multiplicity of behavior," in *Conference on Robot Learning*. PMLR, 2023, pp. 22–31.
- [25] Y. Ji, G. B. Margolis, and P. Agrawal, "Dribblebot: Dynamic legged manipulation in the wild," *arXiv preprint arXiv:2304.01159*, 2023.
- [26] C. Li, S. Blaes, P. Kolev, M. Vlastelica, J. Frey, and G. Martius, "Versatile skill control via self-supervised adversarial imitation of unlabeled mixed motions," in *2023 IEEE International Conference on Robotics and Automation (ICRA)*. IEEE, 2023, pp. 2944–2950.
- [27] J. Wu, G. Xin, C. Qi, and Y. Xue, "Learning robust and agile legged locomotion using adversarial motion priors," *IEEE Robotics and Automation Letters*, 2023.
- [28] R. V. Florian, "Reinforcement learning through modulation of spike-timing-dependent synaptic plasticity," *Neural computation*, vol. 19, no. 6, pp. 1468–1502, 2007.
- [29] M. J. O'Brien and N. Srinivasa, "A spiking neural model for stable reinforcement of synapses based on multiple distal rewards," *Neural Computation*, vol. 25, no. 1, pp. 123–156, 2013.
- [30] M. Yuan, X. Wu, R. Yan, and H. Tang, "Reinforcement learning in spiking neural networks with stochastic and deterministic synapses," *Neural computation*, vol. 31, no. 12, pp. 2368–2389, 2019.
- [31] K. Doya, "Reinforcement learning in continuous time and space," *Neural computation*, vol. 12, no. 1, pp. 219–245, 2000.
- [32] B. Rueckauer, I.-A. Lungu, Y. Hu, M. Pfeiffer, and S.-C. Liu, "Conversion of continuous-valued deep networks to efficient event-driven networks for image classification," *Frontiers in neuroscience*, vol. 11, p. 682, 2017.
- [33] J. H. Lee, T. Delbruck, and M. Pfeiffer, "Training deep spiking neural networks using backpropagation," *Frontiers in neuroscience*, vol. 10, p. 508, 2016.
- [34] W. Fang, Z. Yu, Y. Chen, T. Masquelier, T. Huang, and Y. Tian, "Incorporating learnable membrane time constant to enhance learning of spiking neural networks," in *Proceedings of the IEEE/CVF international conference on computer vision*, 2021, pp. 2661–2671.
- [35] W. Fang, Y. Wang, L. Pang, Z. Gu, Y. Wei, Y. Liu, P. Zhang, C. Chen, X. Zhou, Y. Liu *et al.*, "Lymph node metastasis in thymic malignancies: a chinese multicenter prospective observational study," *The Journal of Thoracic and Cardiovascular Surgery*, vol. 156, no. 2, pp. 824–833, 2018.
- [36] C. Pehle and J. E. Pedersen, "Norse-a deep learning library for spiking neural networks," *Version 0.0*, vol. 6, p. 25, 2021.
- [37] G. Tang, N. Kumar, R. Yoo, and K. Michmizos, "Deep reinforcement learning with population-coded spiking neural network for continuous control," in *Conference on Robot Learning*. PMLR, 2021, pp. 2016–2029.
- [38] G. Tang, N. Kumar, and K. P. Michmizos, "Reinforcement co-learning of deep and spiking neural networks for energy-efficient mapless navigation with neuromorphic hardware," in *2020 IEEE/RSJ International Conference on Intelligent Robots and Systems (IROS)*. IEEE, 2020, pp. 6090–6097.
- [39] Y. Wu, L. Deng, G. Li, J. Zhu, and L. Shi, "Spatio-temporal back-propagation for training high-performance spiking neural networks," *Frontiers in neuroscience*, vol. 12, p. 331, 2018.